EPR study of K_2SeO_4:Cu^{2+} in the high-temperature phase and in the incommensurate phase

G. Zwanenburg, J. J. M. Michiels, and E. de Boer
Research Institute for Materials, University of Nijmegen, Toernooiveld, 6525 ED Nijmegen, The Netherlands
(Received 4 June 1990)

An EPR study of K_2SeO_4 doped with Cu^{2+} in the high-temperature phase and in the incommensurate phase is reported. It was found that only one paramagnetic center is formed. For this center the spin-Hamiltonian parameters in the high-temperature phase were determined. In the incommensurable phase the temperature dependence of a single resonance line was followed as a function of temperature. The temperature dependence of the splitting followed the power law $(T-T_I)^\beta$ with $\beta=0.51$. Furthermore, it was found that in K_2SeO_4:Cu^{2+} the splitting of the resonance lines depends strongly on the nuclear magnetic quantum number m_I.

I. INTRODUCTION

Potassium selenate, K_2SeO_4, is a member of the family of insulators with the general formula A_2BX_4, in which A stands for an alkali-metal ion or other monovalent cation and BX_4 is a tetrahedral divalent anion. Many members of this family exhibit a number of structural phase transitions, some of which involve incommensurable phases. Examples include, in addition to potassium selenate, $Rb_2ZnCl_4(Br_4)$, $[N(CH_3)_4]_2ZnCl_4$, $RbLiSO_4$, and K_2ZnCl_4.[1]

As a typical member of the A_2BX_4 group, K_2SeO_4 has been extensively studied with a number of techniques. X-ray diffraction[2,3] and neutron scattering[4] elucidated the structural phase transitions at $T_I=130$ K and at $T_c=93$ K. At $T=T_I$ a soft phonon with wave vector $\mathbf{q}=\frac{1}{3}(1-\delta)\mathbf{a}^*$ with $\delta\approx0.07$ condenses. The wave length of this phonon is incommensurable with the structure of K_2SeO_4 above T_I. As the temperature is further lowered, δ decreases and at $T=T_c$ the value of q changes discontinuously to $q=\frac{1}{3}$. Below T_c, K_2SeO_4 is ferroelectic with a polarization in the c direction.

Nuclear magnetic resonance of ^{39}K and ^{77}Se (Ref. 5) showed that the potassium atoms are much more susceptible to the structural changes than the selenium atoms. EPR studies of SeO_4^- radicals that were obtained by γ irradiation of crystals K_2SeO_4 showed that phase solitons play an important role in the incommensurable phase of K_2SeO_4.[6,7] The effect of solitons was also observed in the EPR spectra of K_2SeO_4 doped with VO^{2+} ions.[8–10]

Here we report a study of the temperature dependence of the EPR spectra of K_2SeO_4 doped with Cu^{2+} ions. Contrary to the results of a preliminary study by Kobayashi *et al.*,[11] the effect of the phase transiton from the high-temperature phase to the incommensurable phase on the EPR spectra could be observed in the form of a splitting of the high-temperature resonance lines. Since a complete analysis of the EPR spectra in the high-temperature phase has not been given yet, the EPR spectra of K_2SeO_4 in the high-temperature phase are discussed first. The results can be compared with the EPR spectra of Cu^{2+} ions in potassium sulfate, K_2SO_4, and in rubidium sulfate, Rb_2SO_4,[12–14] which are both isomorphous with K_2SeO_4. In the subsequent section the temperature dependence of the spectrum is described as the temperature is lowered below T_I.

II. THE STRUCTURE OF K_2SeO_4

In the high-temperature phase, K_2SeO_4 is isomorphous with β-K_2SO_4, which has space group *Pnam* (D_{2h}^{16}). The unit cell contains four K_2SeO_4 units. There are two crystallographically inequivalent potassium ions per unit cell. One potassium ion, K(1), is surrounded by eleven oxygen atoms. Three of the oxygen atoms are located on the same mirror plane at $z=\frac{1}{4}$, as is K(1), and form an almost regular triangle. The other eight oxygen atoms are positioned above and below the $z=\frac{1}{4}$ mirror plane. In this way, the eleven oxygen atoms provide an almost spherical environment for K(1) in which the average potassium-oxygen distance is about 3.14 Å. The other potassium ion, K(2), is surrounded by nine oxygen atoms at an average potassium-oxygen distance of 2.93 Å. Here also three oxygen atoms share the mirror plane with the potassium ion they surround. The remaining six oxygen atoms are situated above and below the mirror plane.[15]

The selenium atoms are also located on the $z=\frac{1}{4}$ and $z=\frac{3}{4}$ mirror planes, thus the crystallographic mirror planes also act as mirror planes for the selenate groups. Below the phase transition temperature T_I, the high-temperature structure is distorted by the soft phonon that condenses at the phase transition. The SeO_4 tetrahedra are influenced very little by the distortion and can be considered to be rigid bodies. The eigenvector of the soft mode can then be written as a sum of ten symmetry-adapted eigenvectors. Each eigenvector represents a translational and a rotational contribution to the displacements of the SeO_4 groups and a translational contribution to the displacements of the potassium ions. The most important contribution to the modulation, however, comes from a rotation of the SeO_4 groups around the b direction. This rotation is associated with a displacement of the potassium ions in the c direction.[2,3]

III. EPR OF K_2SeO_4:Cu^{2+} IN THE HIGH-TEMPERATURE PHASE

Potassium selenate single crystals were grown by slow evaporation from an aqueous solution of K_2SeO_4 to which about 1mol % $CuSeO_4$ was added. The EPR spectra were measured at X band on a Bruker ESP-300 spectrometer. Rotation of the crystal and the magnet around two mutual perpendicular axes allowed the measurement of EPR spectra in three mutually orthogonal planes without remounting the crystal.

The EPR spectrum of Cu^{2+}, which has electron spin $S=\frac{1}{2}$, consists of four lines due to the hyperfine interaction with the nucleus which has spin $I=\frac{3}{2}$. For an arbitrary orientation of the magnetic field, the EPR spectrum of K_2SeO_4:Cu^{2+} consists of sixteen lines. If the magnetic field is in one of the crystallographic planes, two sets of four lines are observed. The two sets merge into one when the magnetic field is oriented along a crystallographic axis (see Fig. 1). This indicates the presence of only one paramagnetic center. This is in agreement with the preliminary measurements of Kobayashi *et al.*[11] who also found only one center in the same system. It is interesting to note that in the isostructural compound K_2SO_4 doped with Cu^{2+}, three different centers could be identified.[12] In Rb_2SO_4:Cu^{2+} on the other hand, again only one center was found.[13,14]

The width of the resonance lines showed a strong temperature dependence. At room temperature the linewidth is about 2 mT, whereas the linewidth reduces to 0.4 mT at 140 K. Apart from the change in linewidth, the spectra showed no change with temperature in the temperature range between room temperature and 140 K. Because of the significantly better signal-to-noise ratio at 140 K compared to room temperature, the EPR spectra were measured at 140 K.

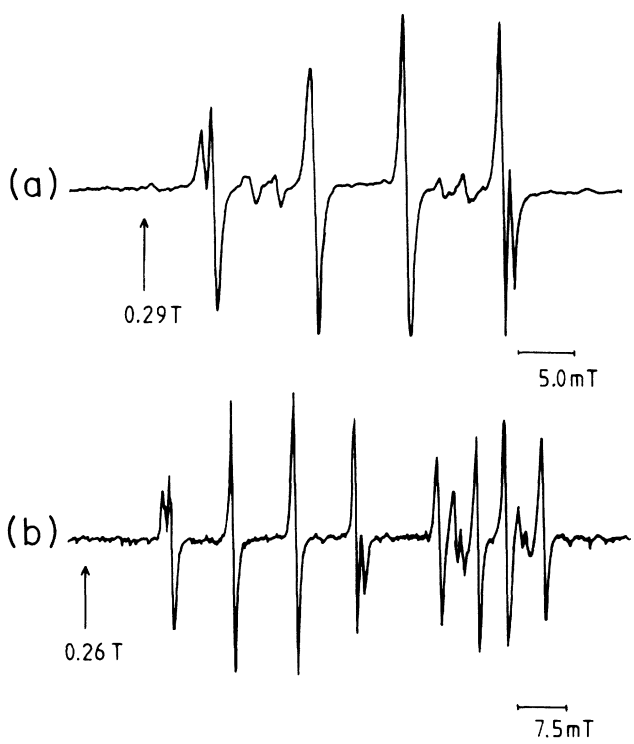

FIG. 1. EPR spectrum of K_2SeO_4:Cu^{2+}. (a) Magnetic field along the a axis; (b) Magnetic field in the ab plane.

TABLE I. Spin-Hamiltonian parameters of $^{63}Cu^{2+}$ in K_2SeO_4. The estimated error in the g values is 0.002, in the hyperfine interaction parameters 1.0×10^{-4} cm^{-1}, and in the quadrupole parameters 0.5×10^{-4} cm^{-1}.

g_1	2.389
g_2	2.148
g_3	2.034
$A_1(10^{-4}$ cm$^{-1})$	118.7
$A_2(10^{-4}$ cm$^{-1})$	45.9
$A_3(10^{-4}$ cm$^{-1})$	23.2
$P_1(10^{-4}$ cm$^{-1})$	5.7
$P_2(10^{-4}$ cm$^{-1})$	−1.1
$P_3(10^{-4}$ cm$^{-1})$	−4.6

The spectra can be described by the spin Hamiltonian

$$H=\beta\mathbf{B}\cdot\mathbf{g}\cdot\mathbf{S}+\mathbf{I}\cdot\mathbf{A}\cdot\mathbf{S}+\mathbf{I}\cdot\mathbf{P}\cdot\mathbf{I}-g_N\beta_N\mathbf{B}\cdot\mathbf{I}\ . \quad (1)$$

The spin-Hamiltonian parameters for the ^{63}Cu isotope were obtained by fitting this spin Hamiltonian to the experimental spectra. The parameters for the other copper isotope, ^{65}Cu, were calculated using the ratio $^{65}g_N/^{63}g_N=1.07$.[16] The error in the fitting was 9 MHz, hence an error of 0.1%. The resulting spin-Hamiltonian parameters for the ^{63}Cu isotope are given in Table I. The angles of the principal axes of the tensors with respect to the crystallographic axes are given in Table II.

The spectra of Fig. 1 were simulated with the spin-Hamiltonian parameters in Table I. The resulting simulations are given in Fig. 2. Both the allowed and first-order forbidden transitions are reproduced very well.

As mentioned above, the number of lines in the EPR spectrum indicates that only one paramagnetic center is present. Assuming the Cu^{2+} ion replaces a K^+ ion, leaving a vacancy at a nearby K^+ position, there are a number of possible Cu^{2+} vacancy combinations. We use some heuristic arguments to show that the Cu^{2+} ion replaces a $K^{2+}(2)$ ion leaving a vacancy at a nearby $K^+(1)$ position.

The direction from the $K^+(2)$ position to the $K^+(1)$ position is given by the angles 71°, 56°, and 40° with the

TABLE II. Angles between the principal axes of the **g**, **A**, and **P** tensor and the crystallographic axes.

	a	b	c
g_1	67	46	53
g_2	29	61	90
g_3	73	59	37
A_1	64	48	53
A_2	70	60	37
A_3	33	57	89
P_1	69	46	52
P_2	39	54	78
P_3	60	66	40

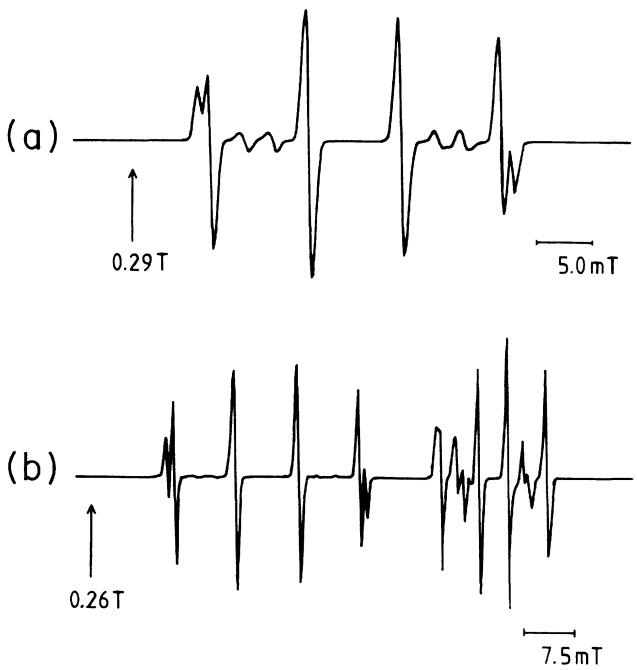

FIG. 2. Simulations of the spectra shown in Fig. 1. (a) Magnetic field along the *a* axis; (b) Magnetic field in the *ab* plane.

crystallographic *a*, *b*, and *c* axes, respectively (see Table II). This direction agrees well with the direction of the g_3 axis. Furthermore, the direction of the g_2 axis is in the *ab* plane and has angles with the *a* and *b* axes of 29° and 61°, respectively. This direction corresponds to the direction of the vector that connects the $K^{2+}(2)$ ion with one of the oxygen atoms in its immediate vicinity.[15]

Based on these considerations, we suggest that the Cu^{2+} ion replaces a $K^+(2)$ ion and that a vacancy is created at the nearest $K^+(1)$ position. This assignment is substantiated by the fact that for the K(2) atoms the average potassium oxygen distance is smaller than for the K(1) atoms, which makes the K(2) position energetically a more favorable place for the Cu^{2+} ion. The same Cu^{2+} vacancy pair was found by Abdulsabirov *et al.*[13] in Rb_2SO_4:Cu^{2+}.

IV. EPR OF K_2SeO_4 IN THE INCOMMENSURABLE PHASE

A. Incommensurable line shape

An EPR spectrum of a single crystal consists of a number of more or less sharp resonance lines. The number of lines reflects the number of magnetically inequivalent sites in the unit cell. In an incommensurable crystal the lattice translation symmetry is lost and all molecules become magnetically inequivalent. In the EPR spectrum this results in a continuous distribution of resonance lines. Therefore, the EPR spectrum of an incommensurable crystal resembles the EPR spectrum of a powder. There are, however, significant differences. The intensity of the resonance line is proportional to the number of paramagnetic ions that is at resonance at a given magnetic field. This number is determined by the rate of change of the magnetic field as a function of position, x. Thus in the case of a one-dimensional modulation:

$$I(B)=C\left[\frac{dB}{dx}\right]^{-1}, \tag{2}$$

with a proportionality constant C. The EPR spectrum is the convolution of the intensity $I(B)$ of the resonance line and a line-shape function $L(B)$:

$$S(B)=\int I(B')L(B-B')dB' . \tag{3}$$

To evaluate the intensity, the relation between the resonance field and the phase of the modulation, $\theta(x)$, must be clarified. The displacement of the atoms from the high-temperature positions is given by the periodic displacement function, $u(x)$, which can be written in terms of the components of the order parameter in the incommensurable phase ρ and $\theta(x)$:

$$u(x)=a_1\rho\cos\theta(x)+a_2\rho\sin\theta(x) , \tag{4}$$

or alternatively,

$$u(x)=A\cos[\theta(x)+\theta_0]\equiv A\cos\phi(x) , \tag{5}$$

where θ_0 depends on the mixing of the two terms in Eq. (4) and A is the amplitude of the modulation. The relation between the resonance field, B, and the displacement function is found by expanding the resonance field in powers of $u(x)$:[17]

$$B=B_0+B_1\cos\phi(x)+\tfrac{1}{2}B_2\cos^2\phi(x)+\cdots , \tag{6}$$

where B_0 is the resonance field in the high-temperature phase, and B_1 and B_2 are expansion coefficients.

In the plane-wave limit $\phi(x)$ is a linear function of x and the displacement function $u(x)$ is

$$u(x)=A\cos(qx+\theta_0) , \tag{7}$$

where q is the wave vector of the modulation. For the intensity one finds

$$I(B)=\frac{C'}{|[B_1+B_2\cos\phi(x)]\sin\phi(x)|} . \tag{8}$$

The edge singularities for this distribution occur at resonance fields

$$B^l=B_0-B_1+\tfrac{1}{2}B_2 , \tag{9}$$

$$B'=B_0+B_1+\tfrac{1}{2}B_2 . \tag{10}$$

Owing to the edge singularities in the line-shape function the incommensurability manifests itself in the EPR spectra by a splitting of the resonance lines. A third singularity may occur for $B_1+B_2\cos\phi(x)=0$ at

$$B^m=B_0-\tfrac{1}{2}B_1^2/B_2 , \tag{11}$$

which would result in an extra line in the EPR spectra.

B. Experimental

The phase transition temperature from the high-temperature phase to the incommensurable phase showed

a considerable hysteresis. On cooling the splitting of the resonance lines due to the incommensurable modulation is observable at about 127 K, whereas on heating the influence of the incommensurability is still observable at 144 K, as is seen in Fig. 3. This figure also shows a fine structure that disappears at about 135 K. This fine structure is too rich to be caused by the incommensurable modulation. To determine the origin of the fine structure, some ENDOR spectra of potassium selenate were recorded. Figure 4 sows typical ENDOR spectra of two paramagnetic sites for an arbitrary orientation of the magnetic field. The spectra unambiguously indicate the presence of protons in the immediate vicinity of the copper ions. These protons must belong to water molecules that are built into the crystal.

To avoid interference of the proton hyperfine splitting with the splitting due to the incommensurable phase, K_2SeO_4 crystals doped with Cu^{2+} were grown from a D_2O solution. In Fig. 5 the experimental and the simulated powder spectra of K_2SeO_4:Cu^{2+} grown from D_2O

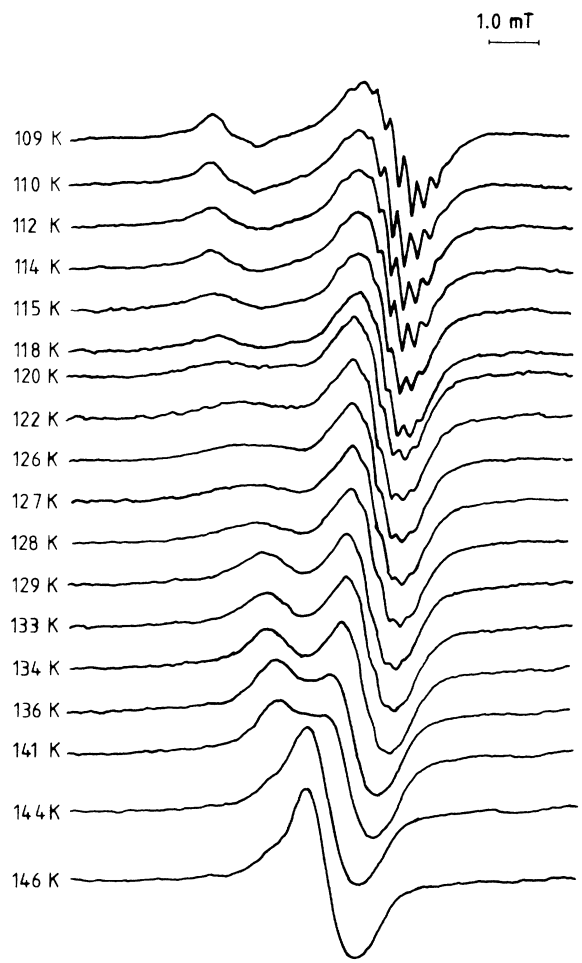

FIG. 3. Temperature dependence of an EPR line of the spectrum of K_2SeO_4 in the incommensurable phase on rising the temperature. The influence of the incommensurable modulation is visible for temperatures up to about 142 K. For temperatures lower than about 135 K a proton hyperfine structure is discernable.

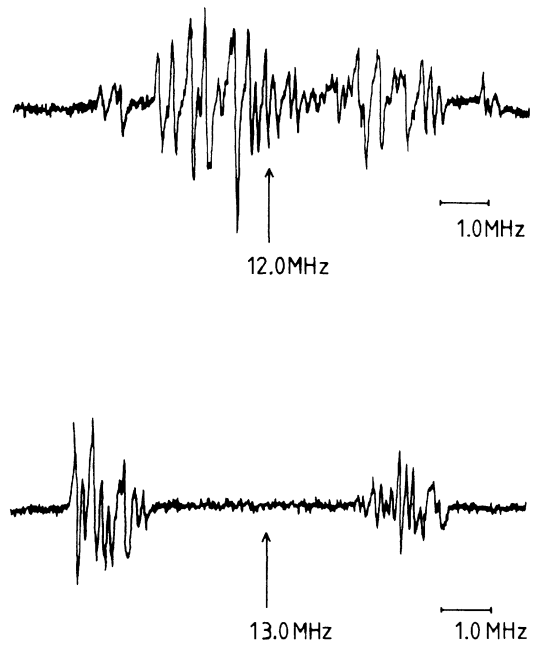

FIG. 4. Proton ENDOR spectra of K_2SeO_4. The spectra were taken for an arbitrary orientation of the magnetic field at $T = 20$ K at two different paramagnetic sites.

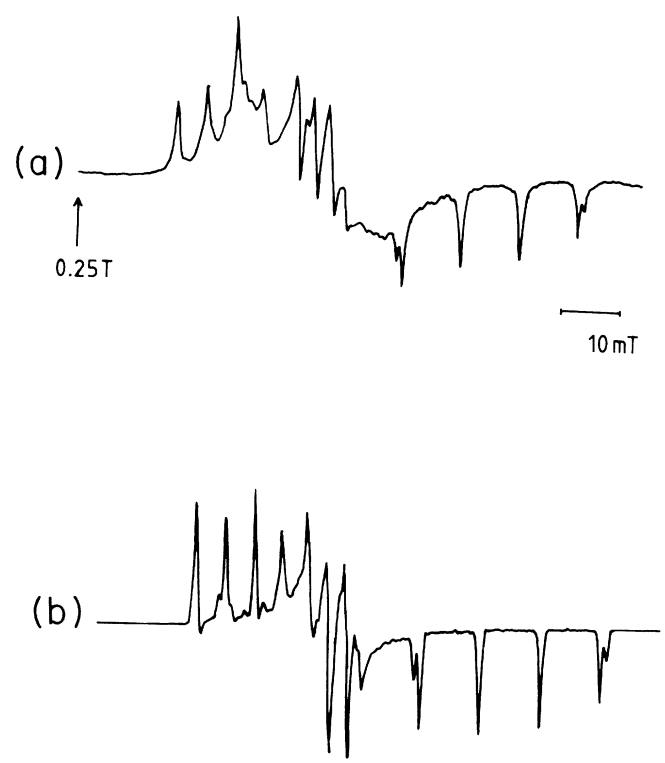

FIG. 5. (a) Powder spectrum of K_2SeO_4 grown from a D_2O solution; (b) Simulated powder spectrum. The simulation was carried out with the spin-Hamiltonian parameters of Table I.

are given. The simulation was carried out with the spin-Hamiltonian parameters as obtained from the crystal grown in H_2O. From the correspondence of the line positions of the experimental and the simulated spectrum, it is concluded that the spin-Hamiltonian parameters are the same for the crystals obtained from H_2O and from D_2O.

Because of the presence of more than one paramagnetic site, the spectra in the incommensurable phase are too complicated to do a full rotational study. Therefore, we concentrate on the temperature dependence of one of the resonance lines. Figure 6 shows part of an EPR spectrum in the incommensurable phase. The lines that are shown are assigned to the $m_I=-\frac{3}{2},-\frac{1}{2},+\frac{1}{2}$ transitions as indicated in the figure. To make this assignment, it is assumed that the hyperfine coupling constant, A, for the Cu^{2+} ion is negative.[18] The line corresponding to the $m_I=-\frac{3}{2}$ transition consists of two sharp lines belonging to the ^{65}Cu and ^{63}Cu isotopes. The splitting of the isotope lines is not visible for the $m_I=\pm\frac{1}{2}$ transitions. The $m_I=-\frac{1}{2}$ line has a slight shoulder on the left side and the $m_I=+\frac{1}{2}$ line is clearly split by the incommensurable modulation. This difference in splittings of the hyperfine lines of the same paramagnetic site can be easily explained if the expansion of the resonance field in terms of the displacements of the atoms from the high-temperature equilibrium positions is considered. The resonance fields of the hyperfine lines in the high-temperature phase are given in first approximation by the expressions

$$h\nu=g\beta B_1-\tfrac{3}{2}A\ ,$$

$$h\nu=g\beta B_2-\tfrac{1}{2}A\ ,$$

$$h\nu=g\beta B_3+\tfrac{1}{2}A\ ,$$

$$h\nu=g\beta B_4+\tfrac{3}{2}A\ ,$$

where g is the effective g value, A the effective hyperfine coupling for the considered magnetic-field orientation, and ν the frequency of the microwave field. In the incommensurable phase, the resonance field is expanded in terms of the displacement, u, of the atoms:

$$B_i=B_{i0}+\left.\frac{\partial B_i}{\partial u}\right|_{u=0}u+\cdots$$
$$=B_{i0}+\frac{h\nu}{\beta}\frac{\partial}{\partial u}\left[\frac{1}{g}\right]\Bigg|_{u=0}u-\frac{m_i}{\beta}\frac{\partial}{\partial u}\left[\frac{A}{g}\right]\Bigg|_{u=0}\times u+\cdots\ , \tag{12}$$

where m_i has the values

$$m_i=\pm\tfrac{1}{2},\pm\tfrac{3}{2}\ . \tag{13}$$

From relation (12) it is seen that depending on the relative signs of $(\partial/\partial u)(1/g)$ and $(\partial/\partial u)(A/g)$, the splitting of the high-field lines is larger or smaller than the splitting of the low-field hyperfine lines. Since the splitting of the high-field line, in our case $m_I=+\frac{1}{2}$, is larger than the splitting of the corresponding low-field line, $m_I=-\frac{1}{2}$ the terms $(\partial/\partial u)(1/g)$ and $(\partial/\partial u)(A/g)$ differ in sign. This phenomenon is also observed in the case of $ThBr_4$:Pa^{4+}.[19]

To follow the temperature dependence of the resonance lines, a single isolated line is chosen to avoid complications due to overlap of multiple lines. The measurements were carried out in a bath cryostat because this allowed a more accurate determination of the temperature of the crystal than in a flow cryostat. The disadvantage of the use of a bath cryostat was that the lowest attainable temperature was about 85 K. Figure 7 shows the temperature dependence of the resonance lines for the ^{63}Cu and ^{65}Cu isotopes corresponding to the $m_I=+\frac{3}{2}$ transition. As the temperature is lowered from $T=142$

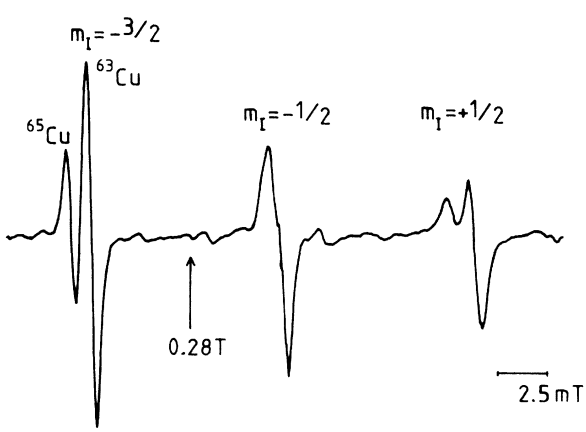

FIG. 6. Part of an EPR spectrum of K_2SeO_4:Cu^{2+} in the incommensurable phase. Shown are the $m_I=-\frac{3}{2},-\frac{1}{2},+\frac{1}{2}$ transitions. The magnitude of the splitting due to the incommensurable modulation depends on the nuclear magnetic quantum number of the transition.

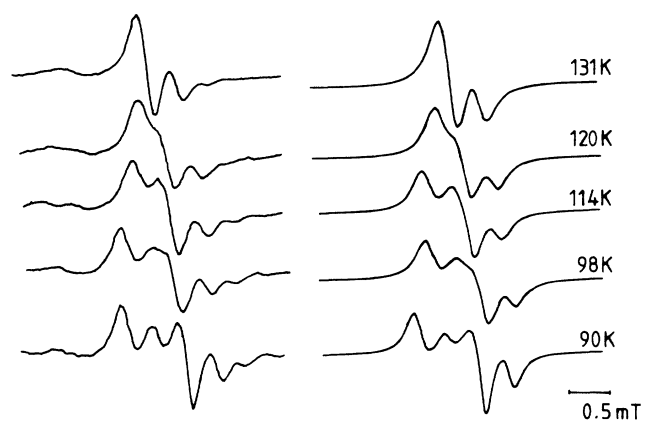

FIG. 7. Temperature dependence of a single resonance line of K_2SeO_4:Cu^{2+} corresponding to the $m_I=+\frac{3}{2}$ transition. The lines of the two copper isotopes can be seen: the high intensity ^{63}Cu line is on the left, the lower intensity ^{65}Cu line is on the right. On the left the experimental spectra are shown; on the right the corresponding simulated spectra.

K, a shoulder becomes visible on the right of the ^{63}Cu line at $T=120$ K. The shoulder develops into a line, corresponding to one of the edge singularities, as the temperature is decreased to 114 K. Upon further cooling an additional line appears between the two edge singularities. This line corresponds to a third singularity in the intensity function $I(B)$ cf. Eq. (11). In Fig. 7 the experimental spectra are given on the left; on the right simulations of the experimental spectra are given. The temperature dependence of the two copper isotope lines could be simulated using as the expression for the resonance field:

$$B=B_0+B_1\cos\phi(x)+\tfrac{1}{2}B_2\cos^2\phi(x)\ . \tag{14}$$

The simulations were calculated by assuming a Lorentzian line-shape function. The resonance fields were calculated for values of ϕ from $\phi=0°$ to $\phi=180°$ in steps of 1°, with B_1 and B_2 as adjustable parameters. Subsequently all the spectra were added.

The temperature dependence of B_1 and B_2 can be written in the form[20]

$$B_1=\left[\frac{T_I-T}{T_I}\right]^{\beta}, \tag{15}$$

$$B_2=\left[\frac{T_I-T}{T_I}\right]^{2\beta}. \tag{16}$$

In Fig. 8, a plot is made of $\log_{10}B_1$ versus $\log_{10}(T_I-T)/T_I$. The B_1 values were obtained from the simulations. From the slope of the line in Fig. 8 it is found that $\beta=0.51$, in excellent agreement with the results of the determination of β from the EPR spectra of VO^{2+} in K_2SeO_4 where $\beta=0.48$ was found.[8] The determination of B_2 from the simulations was not accurate enough to give meaningful results. From the above simulations it can be concluded that K_2SeO_4 can be described by the plane-wave approximation down to $T=90$ K. This was also found in the EPR study of VO^{2+} in K_2SeO_4.[8,9] In the latter study it was found that at temperatures lower than 82 K a multisoliton approximation gave a better explanation of the observed line shape.

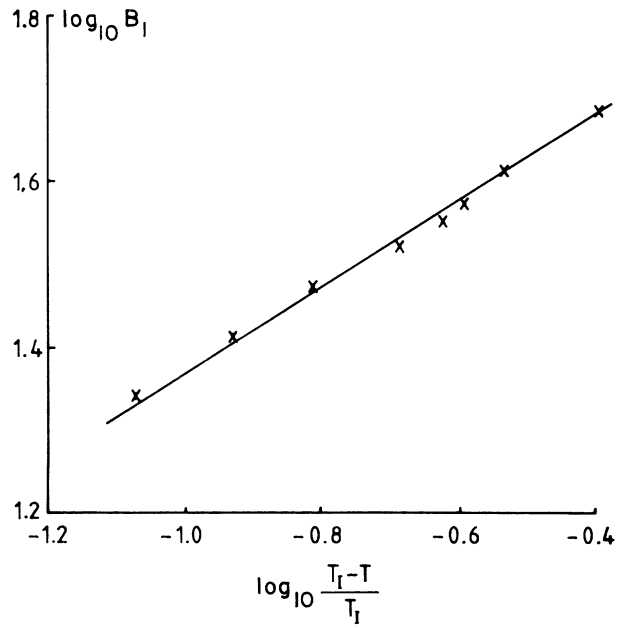

FIG. 8. Plot of $\log_{10}B_1$ vs $\log_{10}(T_I-T)/T_I$. The value of β was obtained from the slope and found to be $\beta=0.51$.

V. CONCLUSIONS

The analysis of the EPR spectra of K_2SeO_4 doped with Cu^{2+} in the high-temperature phase, showed that the Cu^{2+} ions replace one of the potassium ions, leaving a vacancy at the nearest potassium position. Like in Rb_2SO_4 only one type of paramagnetic center is formed in K_2SeO_4.[13]

The spectra in the incommensurable phase could be well explained by assuming a plane-wave modulation in the temperature range from 130 K down to 90 K. An interesting effect that showed particularly clearly in the spectra we measured in the incommensurable phase, is the dependence of the splitting on the nuclear spin quantum number m_I. A more thorough study of this effect may lead to a better understanding of the way the spin-Hamiltonian parameters change with the phase in the modulation wave.

ACKNOWLEDGMENTS

One of the authors (G.Z.) wants to acknowledge the fruitful discussions he had with Dr. R. Kirmse.

[1] *Incommensurate Phases in Dielectrics*, edited by R. Blinc and A. P. Levanyuk (Elsevier, Amsterdam, 1986), Vol. 2.
[2] N. Yamada and T. Theda, J. Phys. Soc. Jpn. **53**, 2555 (1984).
[3] N. Yamada, Y. Ono, and T. Theda, J. Phys. Soc. Jpn. **53**, 2565 (1984).
[4] M. Iizumi, J. D. Axe, and G. Shirane, Phys. Rev. B **15**, 4392 (1977).
[5] B. Topič, A. von Kienlin, A. Goelzauser, U. Haberleben, and R. Blinc, Phys. Rev. B **38**, 8625 (1988).
[6] A. S. Chaves, R.Gazzinelli, and R. Blinc, Solid State Commun. **37**, 123 (1981).
[7] M. S. Dantas, A. S. Chaves, R. Gazzinelli, A. G. Oliveira, M. A. Pimenta, and G. M. Ribeiro, J. Phys. Soc. Jpn. **53**, 2395 (1984).
[8] M. Fukui and R. Abe, Jpn. J. Appl. Phys. **20**, L533 (1981).
[9] M. Fukui and R. Abe, J. Phys. Soc. Jpn. **51**, 3942 (1982).
[10] M. Fukui, C. Takahashi, and R. Abe, Ferroelectrics **36**, 315 (1981).
[11] T. Kobayashi, M. Yakabe, and K. Hukuda, J. Phys. Soc. Jpn. **32**, 578 (1972).

[12]Ya. Abdulsabirov, S. Greznev, and M. M. Zaripov, Sov. Phys. **12**, 509 (1970).
[13]Ya. Abdulsabirov, T. B. Bogatova, Yu. S. Greznev, and M. M. Zaripov, Sov. Phys. **13**, 2091 (1972).
[14]F. E. Freeman and J. R. Pilbrow, J. Phys. C **7**, 2933 (1974).
[15]A. Kálmán, J. S. Stephens, and D. W. Cruickshank, Acta Crystallogr. B **26**, 1451 (1970).
[16]J. E. Wertz and J. R. Bolton, *Electron Spin Resonance* (Chapman and Hall, New York, 1986).
[17]R. Blinc, Phys. Rep. **79**, 331 (1981).
[18]S. K. Misra and C. Wang, Magn. Reson. Rev. **14**, 157 (1990).
[19]C. P. Keijzers, G. Zwanenburg, J. M. Vervuurt, E. de Boer, and J. C. Krupa, J. Phys. C **21**, 659 (1988).
[20]*Incommensurate Phases in Dielectrics,* edited by R. Blinc and A. P. Levanyuk (Elsevier, Amsterdam, 1986), Vol. 1.